Progress In Electromagnetics Research C, Vol. 125, 241–251, 2022

Reconfigurable Hybrid Metal-Graphene UWB Filters for Terahertz Applications

Hamza B. Krid*, Zied Houaneb, and Hassen Zairi

Abstract—This paper presents the design, analysis, and developments of a reconfigurable hybrid metal-graphene filter for terahertz applications. In fact, through the graphene material, we can reconfigure both the resonance frequency and the bandwidth. Further, the variation in chemical potential, relaxation times, and temperature of graphene provides excellent proprieties performances, with a variation of the resonant frequency from 8.60 THz to 8.85 THz, good return loss reaching −22.94 dB, and a bandwidth reconfiguration from 1.717 THz to 1.930 THz. The simulation of the proposed filter is performed using CST software.

1. INTRODUCTION

In recent years, graphene is considered to be a promising future technology in order to replace materials such as copper. As a new material, it is now attracting the attention of researchers around the world for potential especially in the electromagnetic (EM) fields. Actually, the new 2D material has unique thermal, chemical, mechanical, electronic, and optical properties as well as high mobility ($200000\,\mathrm{cm^2v^{-1}s^{-1}}$) [1]. Furthermore, graphene allows varying the chemical potential by polarized voltage, chemical doping, or thermal bias thanks to its exceptional conductivity that can be adjusted to cover a wide frequency range. It also has more confinement, low losses, and better tunability than metal in the THz frequencies [2].

It is possible to manually or automatically change the resonance frequency, operational bandwidth, and radiation pattern of a designed reconfigurable structure (antenna, filter,...) [3]. The most popular reconfiguration methods are electromechanical systems (MEMS or NEMS), electrical RF switches, varactors, tunable materials diode-based technology such as the P-type Insulator N-type diode (PIN diode) or tunable materials using a mechanical, electrical, magnetic, light, and thermal bias [4]. The most significant merit is that the properties of graphene-based antennas can be easily controlled using the electric field effect in the THz frequency. Thus, graphene tunability has been used for small reconfigurable devices in the terahertz regime. Moreover, the reconfiguration of the graphene resistance is an interesting characteristic. In fact, its conductivity can be adjusted to dynamically cover a wide range of domains. Therefore, this material has been widely used for compact reconfigurable systems in terahertz and optical regime. Otherwise, the changing of graphene resistance and applied voltage an intriguing property to microwaves [5, 6]. Therefore, it is often used as miniaturised reconfigurable systems in terahertz, as well as medical and imaging applications [7, 8]. It should be noted that following graphene's groundbreaking impact, the scientific community is actively exploring other two-dimensional semiconductors "beyond graphene," such as Bi_2Se_3 and phosphorene [9], for their prospective application capabilities in nanoelectronics, nanophotonics, and nanomedicine [10]. The increase of wireless communication usage has led the research community to explore new frequency

Received 19 September 2022, Accepted 14 October 2022, Scheduled 25 October 2022
* Corresponding author: Hamza Ben Krid (Hamza.benkrid@eniacar.u-carthage.tn).
The authors are with the Research Laboratory Smart Electricity & ICT, SEICT, National Engineering School of Carthage, University of Carthage, Tunis, Tunisia.

domains in the radio spectrum in order to satisfy the growing needs [11]. That is why the terahertz band [0.1–10 THz] captivated the world community. In fact, this technology is characterized by an unlimited bandwidth, seamless data transfer, microsecond latency, and ultra-fast download that have great impact in revolutionizing the telecommunications domain. In 1970s, the THz term was first used within the microwave domain to describe the water laser resonance, the frequency of interferometers, and the diode detector coverage [12, 13].

The paper is structured as follows. Section 2 will present the proposed design of the filter. Next, Section 3 will be devoted to the modeling and the conductivity of graphene. Section 4, then, will deal with behavior and a comparison between graphene and copper in THz band as well as the results obtained from the reconfiguration using the geometry of the structure and the graphene chemical potential, and the last section summarizes the main conclusions of this paper.

Table 1. Parameters of the proposed filter.

Parameters	Value (μ_m)
Groundplan thickness	0.1
Graphene thickness	0.01
h	0.7
W_1	10
W_2	3.375
W_3	4.2
W_4	3.25
W_5	1.4
L_1	11.6
L_2	6.2
L_3	1.7

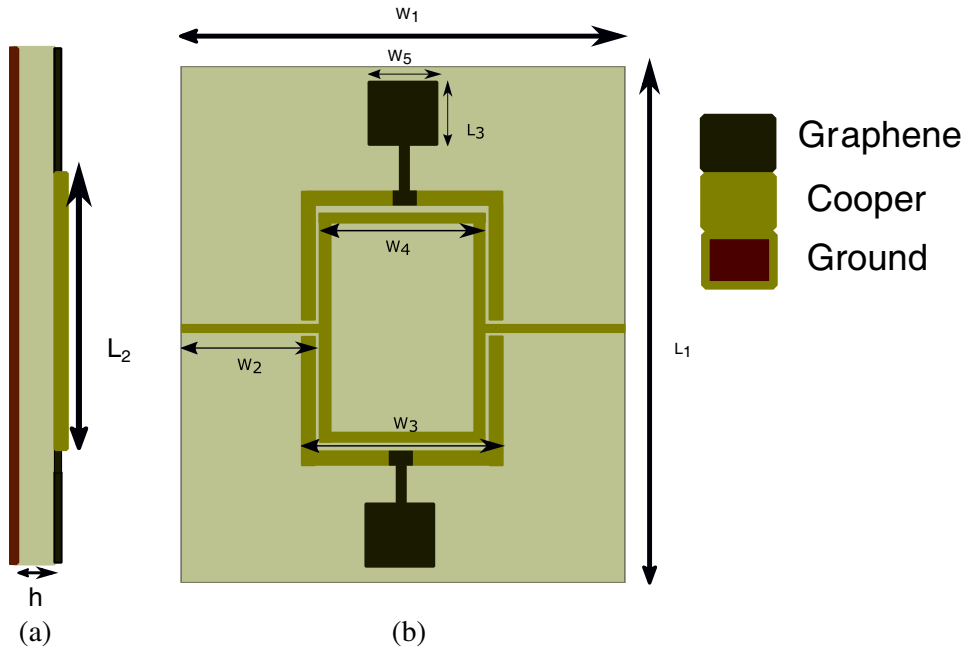

Figure 1. Proposed filter design: (a) side view, (b) top view.

2. DESIGN OF THE PROPOSED FILTER

We design a graphene and copper-based reconfigurable filter. The structure is characterized by a miniaturized size and an ultra-wideband. In order to obtain a bandwidth reconfiguration, we place a copper ring which resonates by coupling effect on two graphene patches. The relative permittivity of the substrate taconic TRF-43 is $\varepsilon = 4,3$, and the structure thickness is of $0.7\mu_t$. Indeed, the rectangular patches are designed with graphene thickness $0.01\mu_t$. The following Table 1 shows the optimized dimensional parameter of the proposed filter.

3. GRAPHENE CONDUCTIVITY

As a 2D material, graphene surface conductivity is expressed by two terms, inter-band and intra-band conductivities. The chemical potential is expressed by substrate thickness and gate voltage as well as controlled by applying and/or doping an electrostatic bias field [14]. Concerning the change in chemical potential, we notice the frequency shift of the imaginary and the real parts of conductivity [15]. The surface conductivity of graphene modeled as a sheet conductor is composed of two terms, one representing the inter-band conductivity and the other denoting the intra-band term [16]. In the terahertz, the surface conductivity band can be expressed using only the first inter-band term and neglecting the second term intra-band, as it has no significant effect [17].

The surface conductivity is as follows [18].

The intra-band conductivity is

$$\sigma_{intra} = -j\frac{e^2 KT_g}{\pi h^2\left(\omega_f - j2\gamma\right)}\left[\frac{\mu_c}{KT_g} + 2\ln\left(e^{-\frac{\mu_c}{KT_g}} + 1\right)\right] \tag{1}$$

The inter-band conductivity is

$$\sigma_{inter} = -j\frac{e^2}{4\pi h}\left[\frac{2\left|\mu_c\right| - (\omega_f - j2\gamma)h}{2\left|\mu_c\right| + (\omega_f - j2\gamma)h}\right] \tag{2}$$

where μ_c is the chemical potential, K the Boltzmann's constant, e the electron charge, T the temperature, h the reduced Planck's, ω_f the angular frequency, and γ the scattering rate. Intra-band conductivity is a complex entity that can be expressed by [14]

$$Res = \mathrm{Re}\left(\frac{1}{\sigma}\right) \tag{3}$$

$$Rea = \mathrm{Im}\left(\frac{1}{\sigma}\right) \tag{4}$$

$$\sigma = \sigma_r + j\sigma_i \tag{5}$$

with σ_r real part of the conductivity and σ_i the imaginary part.

Figures 2 and 3 represent, respectively, the real and imaginary parts of graphene conductivity, as a frequency function related to four different values of the chemical potential 0.1 eV, 0.3 eV, 0.6 eV, and 1 eV. In this context, the temperature is fixed at 300 K, and the relaxation time is selected as 0.1 ps. In addition, the effect of modifying the chemical potential on the conductivity by the polarization voltage control (carrier density) can be seen from the two previous figures.

Figure 4 illustrates the relationship between the bias voltage and the chemical potential, defined by the following equation.

$$\vartheta_g = \frac{h\mu_c^2 e}{\nu_f^2 \varepsilon_0 \varepsilon_r h^2} \tag{6}$$

where ε_r is the permittivity of the substrate, ε_0 the permittivity of free space, h the substrate thickness, and ν_f the Fermi velocity in graphene.

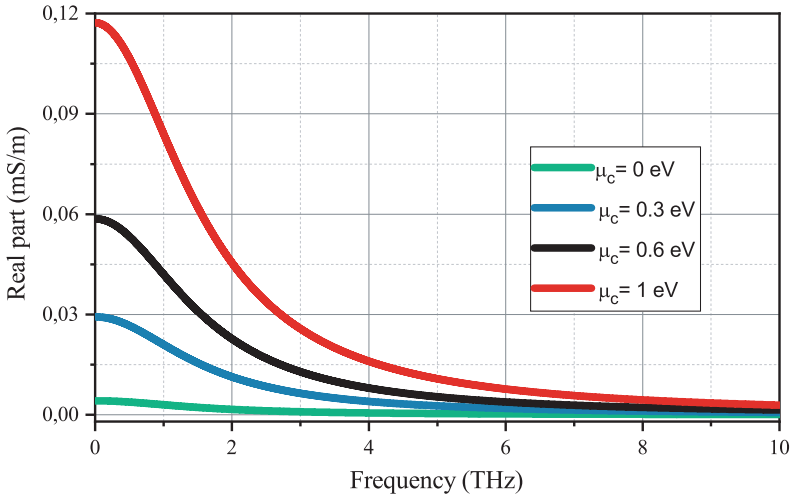

Figure 2. Real part of conductivity.

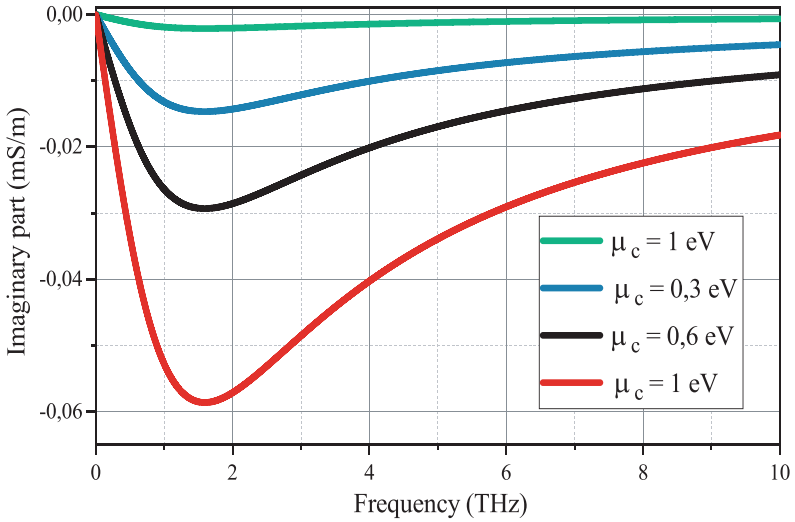

Figure 3. Imaginary part of conductivity.

4. COMPARATIVE BEHAVIOUR STUDY BETWEEN NO-DOPED GRAPHENE AND COPPER

The structure in Figure 1 is simulated by the CST software (Computer Simulation technology). In fact, we consider three chemical potentials, $\mu_c = 0\,\text{eV}$, $\mu_c = 0.2\,\text{eV}$, and $\mu_c = 0.4\,\text{eV}$, in order to reconfigure the resonance frequency and the bandwidth.

4.1. Study of Copper Behavior in Terahertz Band

Copper material is known as an excellent conductor of electricity. In the same way, and it is the most common material in microwave electronics and radio frequency. Despite its high electrical conductivity, it remains unchanged at terahertz frequencies [19]. Likewise, in terahertz band the conductivity and skin depth of copper decrease. At low terahertz frequencies, the copper kinematic inductance is smaller than its ohmic resistance but significantly greater than its internal inductance ($\omega\tau > 1$, where τ is the relaxation time, and ω is the angular frequency). At 6.45 THz, $\omega\tau = 1$, ohmic resistance domination, therefore, it is too difficult to design filters or antennas at THz frequency, generally, due the decrease of conductivity and skin depth [20]. Table 2 summarizes the behavior of the copper in the terahertz band.

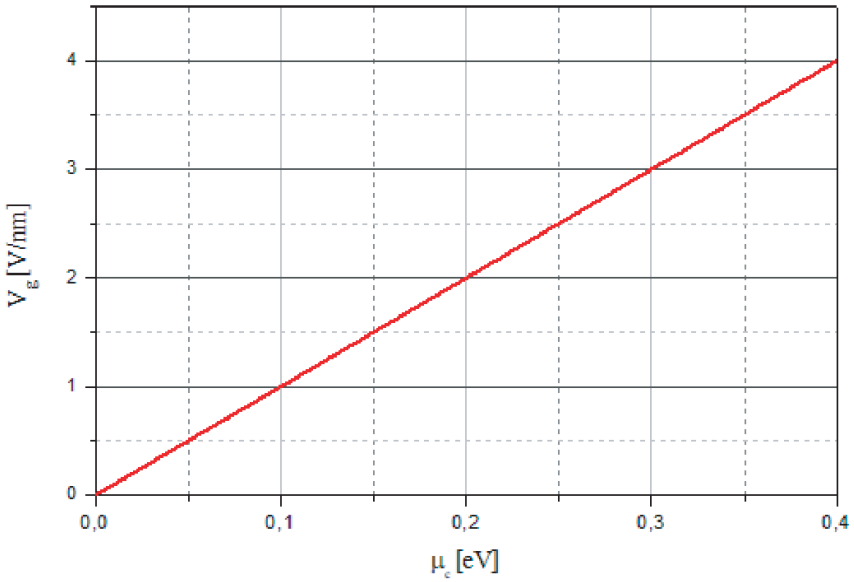

Figure 4. Voltage applied to graphene.

Table 2. Behavior of the copper.

Parameters	Value (μ_m)
Thermal conductivity	$400\,\mathrm{W\,m^{-1}\,K^{-1}}$
Current density	$\sim 10^6\,\mathrm{A\,cm^{-1}}$
Electronic mobility	$32\,\mathrm{cm^2\,V^{-1}\,s^{-1}}$
Tensile strength	587 MPa
Density	$2700\,\mathrm{K_g\,m^{-3}}$

4.2. Study of No-Doped Graphene Behavior in Terahertz Band

The unique optical, thermal mechanical and electronic proprieties of graphene at THz frequency open plethora of applications in many fields. The propagation of surface plasmon polariton is a unique characteristic of graphene at THz frequency. Graphene may be described at THz frequency as an infinite thin conductive sheet with a complicated surface conductivity. The intra-band conductivity, further, dominates over inter-band conductivity in the low THz frequency range. Moreover, at low THz frequency, a single graphene layer provides inductive surface impedance when $x > 1/\tau$. It should be noted that $T = 300\,\mathrm{K}$ and $\tau = 0.5$ are assumed in our work. Owing to supporting low loss plasmonic resonance at THz frequencies, recently, the usage of monolayer and multilayer graphene for THz band and filter applications has been investigated. Furthermore, the surface conductivity of graphene may be modified by means of electrostatic bias or chemical doping, which in turn modifies the characteristics of graphene THz filters and antennas [21]. Table 3 presents the behavior of the graphene in the terahertz band.

4.3. Comparative Behaviour Study between Copper and No-Doped Graphene

The first simulation aims to compare the filter in the case of copper and the same proposed structure replacing the copper by no-doped graphene. Figure 5 represents the reflection coefficient for the two simulated configurations. In fact, we notice that the copper-based filter is less adapted than the no-doped graphene.

Table 3. Behavior of the graphene THz.

Parameters	Value (μ_m)
Thermal conductivity	$5000\,\mathrm{W\,m^{-1}\,K^{-1}}$
Current density	$\sim 10^6\,\mathrm{A\,cm^{-1}}$
Electronic mobility	$\sim 2\times 10^5\,\mathrm{cm^2\,V^{-1}\,s^{-1}}$
Tensile strength	1.5 TPa
Elastic limit	$\sim 20\%$

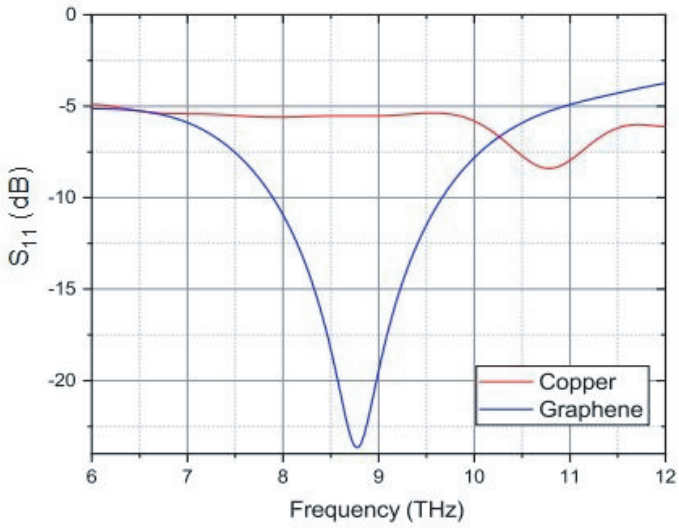

Figure 5. Comparative curves of the return loss S_{11} of no-doped graphene filter and proposed copper filter.

On the other hand, graphene gives better performance in terms of reflection coefficient. The return loss is reduced from -6.440 to -15.125 dB. It is quite reasonable because copper is not used in the THz band order.

Figure 6 shows the surface current distribution of the filter. From this figure we can see that the graphene shows better results.

5. RESULTS AND DISCUSSION

The filter proposed in Figure 1 is simulated and designed by the software CST Electromagnetic. In order to reconfigure the bandwidth and resonance frequency of our structure, we used three different values of the chemical potential μ_c (0, 0.2, 0.4 eV). There are three resonance frequencies which are 8.60, 8.75, 8.85 THz, for each value of the chemical potential and a bandwidth which covers the range from 1.717 THz to 1.930 THz. Figure 7 and Figure 8 represent, respectively, the transmission coefficient and reflection coefficient for the different values of the chemical potential.

To obtain the reconfiguration of the bandwidth and resonance frequency, it is necessary to switch the value μ_c. For the first value of $\mu_c = 0$ eV, we obtain a resonance frequency $fr_1 = 8.60$ THz and BW1 = 1.717 THz (7.753–9.470 THz). For the second value of $\mu_c = 0.2$ eV, we obtain a resonance frequency $fr_2 = 8.75$ THz and BW2 = 1.810 THz (7.869–9.679 THz). The bandwidth is increased by 93 GHz, and the return loss is reduced from -21.067 dB to -22.94 dB. Concerning the last value of $\mu_c = 0.4$ eV, we obtain resonance frequency $fr_3 = 8.85$ THz and BW3 = 1.930 THz (7.853–9.783 THz). The bandwidth is increased by 120 GHz, and the return loss is reduced from -22.94 dB to -23.91 dB.

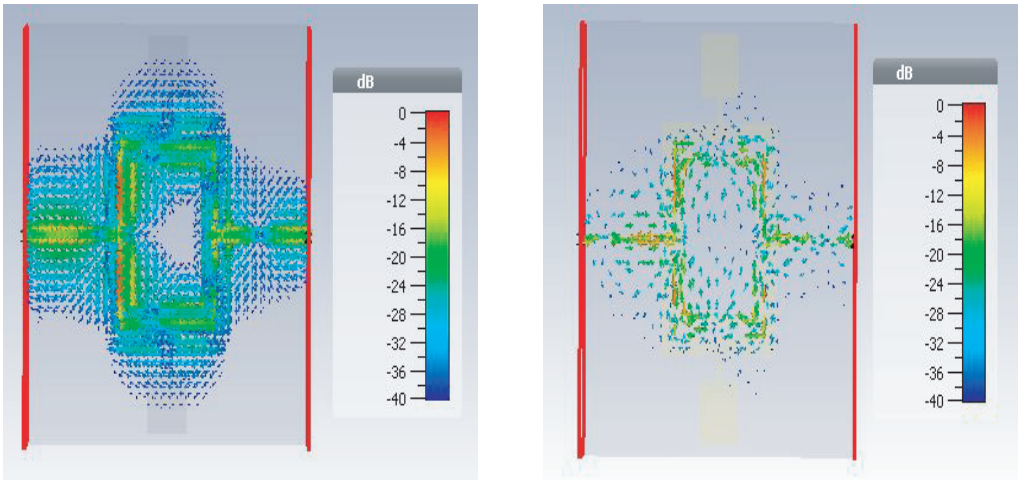

(a) (b)

Figure 6. Current distribution surface: (a) graphene, (b) copper.

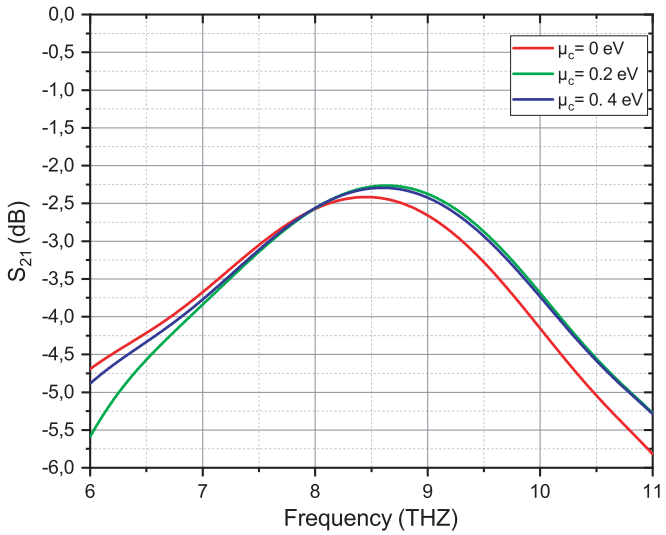

Figure 7. Transmission coefficient for the different values of the chemical potentials.

Table 4. Performance of the proposed antenna for various chemical potential value.

μ_c (eV)	f_r (THz)	BW (THz)	Return loss (dB)
$\mu_c = 0$	8.60	1.717	21.07
$\mu_c = 0.2$	8.75	1.810	22.94
$\mu_c = 0.4$	8.85	1.930	23.91

From Table 4, it can be seen that by tuning the proposed filter, the resonant frequency varies from 8.60 THz to 8.85 THz, and the BW increases from 1.717 THz to 1.930 THz. Also, a second observation is that as the value of chemical potential increases, the filter becomes more adaptable from -21.067 dB to reach -23.91 dB. We notice, in addition, that the best conditions are achieved with 0.4 eV for the

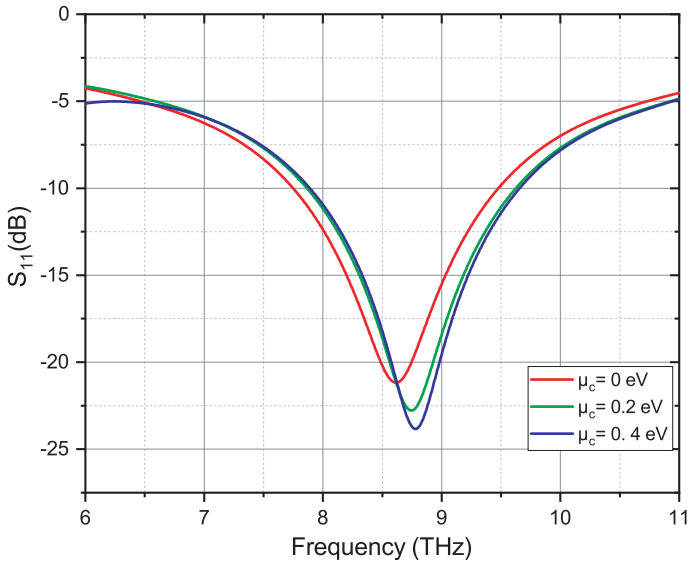

Figure 8. Reflection coefficient for the different values of the chemical potentials.

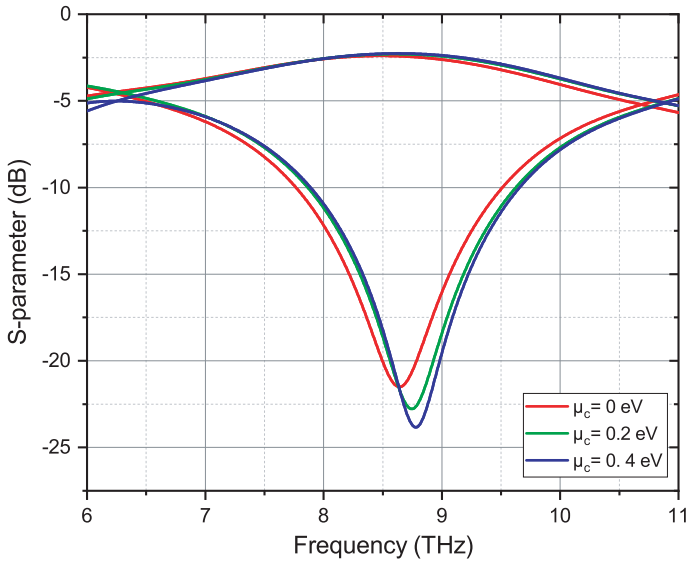

Figure 9. *S*-parameters for the different values of the chemical potentials.

chemical potential.

In Figure 9, as the chemical potential varies from 0 to 0.4 eV, the positions of bandwidth and resonance frequency vary too. Other parameters are the temperature and relaxation time of graphene, which are studied, respectively, in Figure 10.

From Figure 11(a) we can note that, as the temperature of graphene varies from 200 K to 400 K, the positions of bandwidth and resonance frequency are tuned of 0.46% and 1.34%.

Like in Figure 11(b) we can recognize that, as the relaxation time of graphene varies from 0 ps to 1 ps, the positions of bandwidth and resonance frequency are tuned of 0.46% and 0.67%, respectively.

The performance comparisons between previous based graphene filters and this work are listed in Table 5. As we can see the proposed filter has the characteristic of broad bandwidth and also a low return loss compared to [22].

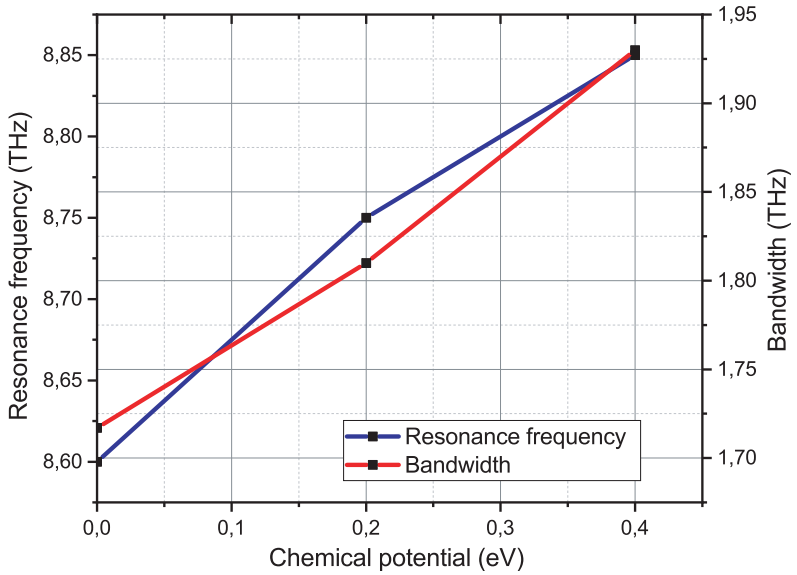

Figure 10. Variation of resonance frequency and bandwidth vs different values of chemical potentiel.

Table 5. Performance comparison of this work and previous based graphene filter.

References	S_{21} (dB)	S_{11} (dB)	BW (THz)	Structure
[22]	< -5	< -20	0.63	Graphene+ S_iO_2
[23]	< -5	< -50	0.2	Graphene+ Duroid
This work	< -10	< -30	1.71	Hybrid graphene/metal + TRF-43

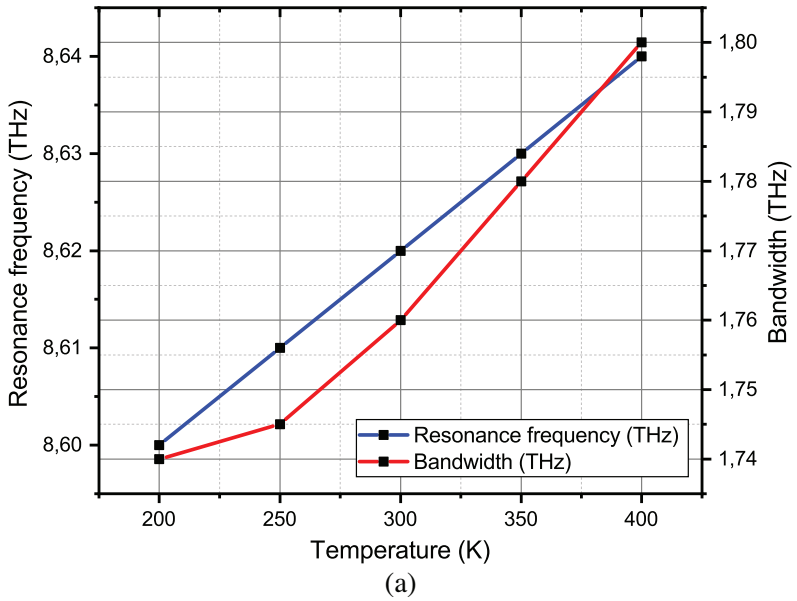

(a)

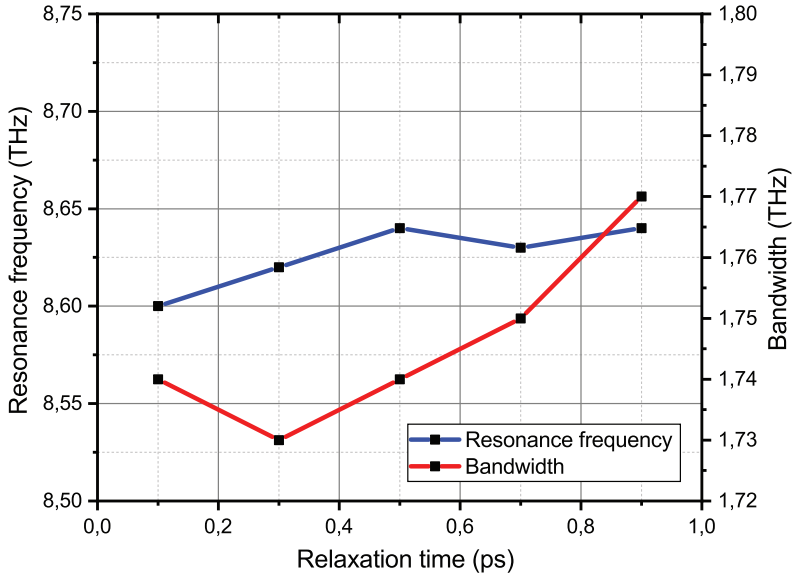

(b)

Figure 11. Proposed filter design: (a) Variation of resonance frequency and bandwidth vs different values of temperature, (b) Variation of resonance frequency and bandwidth vs different values of relaxation time.

6. CONCLUSIONS

In this paper, a graphene filter intended for terahertz medical application is proposed. According to the comparison between the copper and graphene, the new material gives a tunable results in terms of bandwidth varying between 1.717 THz and 1.930 THz. In other words, graphene showed better results in terms of performances with a good adaptation. In order to investigate the effect of the relaxation time, temperature, and chemical potential, we use the CST software.

REFERENCES

1. Kuman, A., K. Sharma, and A. Dixit, "A review of the mechanical and thermal properties of graphene and its hybrid polymer nanocomposites for structural applications," *Journal of Materials Science*, Vol. 52, 5992–6026, 2019.
2. Das, S., Y. S. Kang, and A. Dixit, "Graphene synthesis and application for solar cells," *Journal of Materials Research*, Vol. 29, 299–319, 2014.
3. Costantine, J., et al., "Reconfigurable antenna design and application," *Proceeding of the IEEE*, Vol. 103, 424–437, 2015.
4. Azizi, M. K., M. A. Ksiksi, H. Ajlani, and A. Gharsallah, "Terahertz graphene-based reconfigurable patch antenna," *Progress In Electromagnetics Research Letters*, Vol. 71, 69–76, 2017.
5. Ullah, Z., G. Witjaksono, et al., "A review on the development of tunable graphene nanoantennas for terahertz optoelectronic and plasmonic applications," *Sensors*, Vol. 20, 1401, 2020.
6. Serrano, D. S. and J. S. Diaz, "Graphene-based antennas for terahertz systems: A review, forum for electromagnetic research methods and application technologies," 1–26, 2017.
7. Khan, M., M. Abdul Kaium, and T. Ahmed, "A Graphene patch antennas with different substrate shapes and materials," *International Journal for Lights and Electron Optics*, Vol. 202, 163700, 2020.

8. Najafi, A., M. Soltani, and I. Chaharmahali, "Reliable design of THz absorbers based on graphene patterns: Exploiting genetic algorithm," *International Journal for Lights and Electron Optics*, Vol. 203, 163924, 2020.
9. Leonardo, V., H. Jin, et al., "Efficient terahertz detection in black-phosphorus nano-transistors with selective and controllable plasma-wave, bolometric and thermoelectric response," *Scientific Reports*, Vol. 6, 1–23, 2016.
10. Tang, W., A. Politano, et al., "Ultrasensitive room-temperature terahertz direct detection based on a bismuth selenide topological insulator," *Advanced Functional Materials*, 1–23, 2018.
11. Elyan, H., O. Amin, et al., "Terahertz band: The last piece of RF spectrum puzzle communications," *Open Journal on Society IEEE*, Vol. 1, 1–32, 2019.
12. Moon, K., I. Lee, et al., "Nano-gap electrode large area THz emitter for the enhanced emission efficiency and heat dissipation," *IEEE 39th International Conference on Infrared Millimeter and Terahertz Waves*, 1–2, 2014.
13. Keshwala, U., S. Rawat, and K. RAy, "Design and analysis of DNA shaped antenna for terahertz and sub-terahertz applications," *International Journal for Lights and Electron Optics*, Vol. 232, 166512, 2021.
14. Krid, H. B., Z. Houaneb, and H. Zairi, "Dual-band reconfigurable graphene antenna for THz applications," *4th International Conferance on Advanced Systems and Emergent Technologies (IC-ASET)*, 79–82, 2020.
15. Hlali, A., Z. Houaneb, and H. Zairi, "Tunable filter based on hybrid metal-graphene structures over an ultrawide terahertz and using an improved wave concept iterative process method," *International Journal for Light and Electron Optics*, Vol. 181, 423–431, 2018.
16. Hossain, M., M. Muktadhir, and Md. Masud Rana, "Modeling graphene macroscopic and microscopic conductivity in the sub-cell FDTD method," *International Conference on Electrical & Electronic Engineering (ICEEE)*, 53–56, IEEE, 2015.
17. Krid, H. B., Z. Houaneb, H. Zairi, A. Hlali, Z. Houaneb, and H. Zairi, "Reconfigurable graphene annular ring antenna for medical and imaging applications," *Progress In Electromagnetics Research M*, Vol. 89, 53–62, 2020.
18. Hlali, A., Z. Houaneb, and H. Zairi, "Tunable attenuator based on hybrid graphene-black phosphorus microstrip line for terahertz applications," *International Journal for Light and Electron Optics*, Vol. 2021, 164827, 2020.
19. Dash, S. and A. Patnaik, "Material selection for THZ antennas," *Microwave and Optical Technology Letters*, Vol. 60, 1183–1187, 2018.
20. Mbayachi, V. B., E. Ndayiragije, et al., "Graphene synthesis characterization and its applications: A review," *Results in Chemistry*, Vol. 3, 100163, 2021.
21. Wei, X., T. Lv, et al., "A graphene-metamaterial hybrid structure for the design of reconfigurable low pass terahertz filters," Vol. 63, No. 3, 817–882, 2020.
22. Joshi, N. and P. Pathak, "Concurrent dual-band tunable graphene based band-pass filter," *11th International Conference on Industrial and Information Systems (ICIIS)*, 218–223, IEEE, 2016.
23. Zhai, M., H. Peng, et al., "Modeling tunable graphene-based filters using leapfrog ADI-FDTD method," *IEEE MTT-S International Microwave Workshop Series on Advanced Materials and Processes for RF and THz Applications (IMWS-AMP)*, 1–3, IEEE, 2015.